OPEN

# Histology and Gadolinium Distribution in the Rodent Brain After the Administration of Cumulative High Doses of Linear and Macrocyclic Gadolinium-Based Contrast Agents

*Jessica Lohrke, PhD,* Anna-Lena Frisk, PhD,† Thomas Frenzel, PhD,* Laura Schöckel, PhD,‡ Martin Rosenbruch, PhD,§ Gregor Jost, PhD,* Diana Constanze Lenhard, PhD,|| Martin A. Sieber, PhD,¶ Volker Nischwitz, PhD,# Astrid Küppers,# and Hubertus Pietsch, PhD**

**Objectives:** Retrospective studies in patients with primary brain tumors or other central nervous system pathologies as well as postmortem studies have suggested that gadolinium (Gd) deposition occurs in the dentate nucleus (DN) and globus pallidus (GP) after multiple administrations of primarily linear Gd-based contrast agents (GBCAs). However, this deposition has not been associated with any adverse effects or histopathological alterations. The aim of this preclinical study was to systematically examine differences between linear and macrocyclic GBCAs in their potential to induce changes in brain and skin histology including Gd distribution in high spatial resolution.

**Materials and Methods:** Fifty male Wistar-Han rats were randomly allocated into control (saline, n = 10 rats) and 4 GBCA groups (linear GBCAs: gadodiamide and gadopentetate dimeglumine, macrocyclic GBCAs: gadobutrol and gadoteridol; n = 10 rats per group). The animals received 20 daily intravenous injections at a dose of 2.5 mmol Gd/kg body weight. Eight weeks after the last GBCA administration, the animals were killed, and the brain and skin samples were histopathologically assessed (hematoxylin and eosin; cresyl violet [Nissl]) and by immunohistochemistry. The Gd concentration in the skin, bone, brain, and skeletal muscle samples were analyzed using inductively coupled plasma mass spectroscopy (ICP-MS, n = 4). The spatial Gd distribution in the brain and skin samples was analyzed in cryosections using laser ablation coupled with ICP-MS (LA-ICP-MS, n = 3). For the ultra-high resolution of Gd distribution, brain sections of rats injected with gadodiamide or saline (n = 1) were assessed by scanning electron microscopy coupled to energy dispersive x-ray spectroscopy and transmission electron microscopy, respectively.

**Results:** No histological changes were observed in the brain. In contrast, 4 of 10 animals in the gadodiamide group but none of the animals in other groups showed macroscopic and histological nephrogenic systemic fibrosis–like skin lesions. The Gd concentrations observed in the skin/brain samples (in nanomole Gd per gram of tissue) for each agent were as follows: gadodiamide: 1472 ± 115/11.1 ± 5.1, gadopentetate dimeglumine: 80.8 ± 6.2/13.1 ± 7.3, gadobutrol: 1.1 ± 0.5/0.7 ± 0.4, and gadoteridol: 1.7 ± 0.8/0.5 ± 0.2. The average detected residual Gd concentration in the brain was approximately 15-fold higher for linear than for macrocyclic GBCAs. The highest amounts of Gd found in brain corresponded to less than 0.0002% of the injected dose per gram of tissue. Using LA-ICP-MS, high Gd concentrations in the deep cerebellar nuclei and in the granular layer of the cerebellar cortex were detected only for linear gadodiamide and gadopentetate dimeglumine but not for gadoteridol or gadobutrol. The energy dispersive x-ray spectroscopy analysis revealed Gd-containing spots in the skin of animals administered gadodiamide and gadopentetate dimeglumine. Transmission electron microscopy revealed several Gd-containing spots in the region of the dentate nuclei in the brain of 1 animal injected with gadodiamide.

**Conclusions:** After repeated high dosing, nephrogenic systemic fibrosis–like macroscopic and histopathological lesions of the skin were observed only in some of the gadodiamide-treated animals. No histopathological findings were detected in the rodent brain. The administration of linear GBCAs was associated with significantly higher Gd concentrations in the brain and skin compared with macrocyclic GBCA administration. The results of LA-ICP-MS demonstrated local accumulation of Gd within the deep cerebellar nuclei and the granular layer only after the administration of linear agents. In summary, the detected low Gd concentrations in the skin and brain were well correlated with the higher kinetic stability of macrocyclic GBCA.

**Key Words:** contrast agent, gadolinium retention, MRI, dentate nucleus, globus pallidus, histology, gadobutrol, gadodiamide, gadopentetate dimeglumine, gadoteridol

(*Invest Radiol* 2017;52: 324–333)

Gadolinium-based contrast agents (GBCAs) are of great value for diagnostic magnetic resonance imaging (MRI) and are widely used in clinical routine. With more than 460 million procedures performed to date, contrast-enhanced MRI is a well-established, safe, and valuable diagnostic imaging technique that is used worldwide.[1] Gadolinium (Gd), dissociated from its ligand and present as a new Gd species, can have adverse biological effects. Therefore, the Gd ion is tightly bound to a high affinity ligand when used as a contrast agent. Based on the chemical structure of this ligand, GBCAs can be divided into 2 different classes: linear and macrocyclic. The major difference between the 2 classes is their kinetic inertness[2] and propensities to release Gd in vivo and potential to trigger nephrogenic systemic fibrosis (NSF),[3] a serious syndrome that involves fibrosis of the skin and the internal organs affecting patients with renal dysfunction.[4,5] While macrocyclic GBCAs are extremely stable and basically inert under physiological conditions,[2,6] linear GBCAs are characterized by a lower complex stability and are associated with NSF.[3,7]

Several retrospective studies in patients with primary brain tumors or other central nervous system (CNS) pathologies have reported increased signal intensities (SIs) in the dentate nucleus (DN) and globus

Received for publication October 11, 2016; and accepted for publication, after revision, November 15, 2016.

From the *MR and CT Contrast Media Research, †Research Pathology Berlin, and ‡Medical and Clinical Affairs Radiology, Bayer AG, Berlin; §Special Histopathology, Bayer AG, Elberfeld; ||Institute of Vegetative Physiology, Charité; ¶Clinical Project Management, Bayer AG, Berlin; and #Central Institute for Engineering, Electronics and Analytics (ZEA-3), Forschungszentrum Juelich GmbH, Juelich, Germany.

Conflicts of interest and sources of funding: J.L., A.L.F., T.F., L.S., G.J., M.R., and M.A.S. are employees of Bayer AG. D.C.L. received a research grant from Bayer AG. Forschungsinstitut Juelich GmbH received a grant for Laser ablation-ICP-MS measurements contractually settled in a laboratory service agreement.

Supplemental digital contents are available for this article. Direct URL citations appear in the printed text and are provided in the HTML and PDF versions of this article on the journal's Web site (www.investigativeradiology.com).

Correspondence to: Hubertus Pietsch, PhD, MR and CT Contrast Media Research, Bayer AG, Muellerstrasse 178, 13353 Berlin, Germany. E-mail: hubertus.pietsch@bayer.com.



ISSN: 0020-9996/17/5206–0324
DOI: 10.1097/RLI.0000000000000344

pallidus (GP) based on unenhanced T1-weighted MRIs in patients after multiple applications of primarily linear GBCAs.[8–17] Histopathological correlation studies in postmortem brain tissues have suggested a correlation between an SI increase and Gd deposition in the DN and GP.[10,18] Notably, to date, these findings have not been associated with any clinical symptoms or adverse health effects. However, several publications do suggest a potential correlation.[19,20] At this time, none of these publications provide any reasonable scientific evidence of a causal association.

Systematic evaluations of potential Gd deposition under controlled and reproducible conditions, similar to other mechanistic preclinical toxicity studies, have confirmed the clinical observations of brain signal hyperintensities of retrospective patient studies.[21–23]

The purpose of the present study was to determine the potential correlation of histopathological changes and Gd distribution in rodent brain and skin samples after multiple administrations of either linear or macrocyclic GBCAs. In addition, the specific distribution of Gd in brain and skin tissue was assessed using highly sensitive laser ablation inductively coupled plasma mass spectrometry (LA-ICP-MS), and the semi-thin and ultra-thin sections of the brain samples of gadodiamide or saline-treated animals were assessed using scanning electron microscopy coupled to energy dispersive x-ray spectroscopy (SEM-EDX) and transmission electron microscopy (TEM-EDX), respectively.

## MATERIALS AND METHODS

### Contrast Agents

Four different commercially available GBCAs were investigated (2 linear and 2 macrocyclic GBCAs): gadopentetate dimeglumine (Magnevist; Bayer Vital GmbH, Leverkusen, Germany), gadodiamide (Omniscan; GE Healthcare Buchler GmbH & Co KG, Braunschweig, Germany), gadoteridol (Prohance; Bracco Imaging Deutschland GmbH, Konstanz, Germany), and gadobutrol (Gadovist; Bayer Vital GmbH, Leverkusen, Germany).

### Animals

Wistar-Han (Crl:WI) rats (males; 250–300 g) were purchased from Charles River (Sulzfeld, Germany). The animals were maintained under standard laboratory conditions at a temperature of 22°C and a dark/light cycle of 12 hours. Standard food and water were provided ad libitum. The animals were handled in compliance with German animal welfare legislation, and the experiments were performed with the approval of the state animal welfare committee.

### Study Setup

Fifty rats were randomly allocated to control and 4 GBCA groups (n = 10 per group). The animals received 20 intravenous injections each at a dose of 2.5 mmol Gd/kg body weight for 5 consecutive days per week over period of 4 weeks (representing 500-fold of the total single dose in humans and more than the 80-fold of the surface-adapted standard dose). All injections were performed on conscious animals. Eight weeks after the last injection, the animals were killed under general isoflurane anesthesia. Each animal was rapidly exsanguinated by incision of the jugular blood vessels followed by a full postmortem examination. Tissue samples were collected and followed by histology (n = 3 per group, for n = 1 additional SEM-EDX and TEM-EDX), ICP-MS measurements (n = 4 per group), and laser ablation ICP-MS measurements (n = 3 per group) (Fig. 1).

### Histology

The organs were immersion fixed in neutral-buffered 10% formalin. After routine dehydration, the organs were embedded in paraffin and sectioned (4–6 μm) for hematoxylin and eosin (H&E) staining. Seven full-face coronal (transverse) slices were prepared from each animal using defined gross anatomic landmarks on the ventral aspect of the brain. The cutting microtome blades (Typ S35; Feather, Osaka, Japan) were oriented using a rat brain matrix (RBM-4000C; ASI Instruments, Warren, MI) according to the Society of Toxicologic Pathology position paper.[24]

The following key nervous system brain structures were microscopically examined in H&E-stained sections from 7 slices throughout the brain: olfactory bulb, caudate/putamen, cerebral cortex, corpus callosum, GP, subfornical organ, hippocampus, thalamus, hypothalamus, choroid plexus, pyramids, cerebellum, trigeminal nuclei and tracts, lateral (dentate) cerebellar nuclei (lateral DN), and medulla oblongata. In addition, serial sections were prepared from selected brain sections (brain II and VI where the GP, subfornical organ, and lateral DN are located) for special staining, immunohistochemistry, and SEM-EDX examination. Cresyl violet stains for Nissl bodies, which in normal neurons are composed of rough endoplasmatic reticulum intermingled with myriad polyribosomes and widely disseminated in the cytoplasm, were used to facilitate detection.[25,26] In injured neurons, the Nissl bodies undergo partial to complete dissolution, thus releasing ribosomes needed to manufacture new proteins required to repair the damaged cell infrastructure. A polyclonal rabbit anti-glial fibrillary acidic protein (GFAP) antibody (Dako Z0334, at 1.16 μg/mL) was used to assess astrocyte number and morphology. Resident astrocytes respond regarding a retention of metabolic byproducts/fluid by expansion of cytoplasm and/or membrane-bound organelles and by proliferation to repair tissue defects.[26] The astrocyte end-feet projections interact with endothelial cells by encircling the abluminal side making up an important part of the blood-brain barrier (BBB).[27] A polyclonal goat anti-ionized calcium-binding adapter molecule 1 (Iba1) antibody (Abcam ab5076 at 0.625 μg/mL) was used to identify early activation of microglia (the resident phagocytic cells of the CNS), because microglial response to neuronal damage, culminating in phagocytosis of the degenerating neurons.

Heat-induced antigen retrieval (HIER; citrate buffer pH 6.0, pressure cooker) was applied, followed by incubation with the respective primary antibodies, which were detected using EnVision + System HRP from Dako (4002/K4003) for the GFAP antibody, and a biotinylated polyclonal rabbit anti-goat secondary antibody was used for Iba1, followed by visualization using 3,3′-diaminobenzidine as a chromogenic substrate. European Board–certified veterinary pathologists performed the histopathological evaluation according to the best practice guidelines of the Society of Toxicologic Pathology.[28] Masked evaluation was not implemented because there is no known outcome, defined spectrum of lesions or targets after administration of GBCAs to be identified; in blinded studies, only changes considered to be clearly outside of any reference range can be recorded, reducing the sensitivity of the study.[29]

### ICP-MS Measurements

For quantitative measurements, 7 full-face coronal slices (n = 7 per animal, n = 4 animals per group) of the brain were prepared as described previously. The Gd concentrations in the skin, the bones (femur), the muscles, and the 7 brain slices were determined using inductively coupled plasma mass spectrometry (ICP-MS Agilent 7900; Waldbronn, Germany) to measure the most abundant isotope, $^{158}Gd$. The samples were weighed (~20 mg), cut into pieces and homogenized in microcentrifuge tubes (1.5 mL, Eppendorf Safe-Lock, Sigma-Aldrich Chemie GmbH, Taufkirchen, Germany), mixed with 50 μL of 100 nM $Tb(NO_3)_3$ as an internal standard and dried for 2 hours at 95°C. Subsequently, 50 μL of concentrated nitric acid (65% $HNO_3$, Suprapur; Merck KgaA, Darmstadt, Germany) and 20 μL of hydrogen peroxide ($H_2O_2$, Emsure; Merck KgaA, Darmstadt, Germany) were added, and the samples were heated to dissolve the tissue for 2 hours at 95°C in a microwave oven (MDS 2000; CEM, Kamp-Lintfort, Germany). The diluted samples, standards, and blank samples were measured in triplicate. The limit of quantification was 0.005 nmol Gd/g tissue.

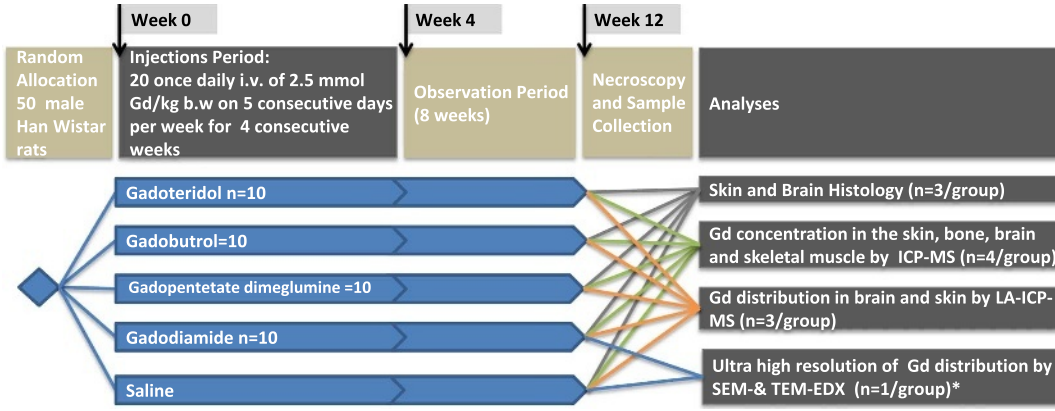


**FIGURE 1.** Schematic illustration of the study design. Healthy male Wistar-Han rats were randomly allocated into 1 control and 4 GBCA groups n = 10 (saline, gadodiamide, gadopentetate dimeglumine, gadobutrol, gadoteridol). Each animal received 20 daily intravenous injections at a dose of 2.5 mmol Gd/kg body weight. Eight weeks after the last application, the animals were killed, the histology and Gd distribution (LA ICP-MS and SEM-EDX and TEM-EDX) were investigated, and ICP-MS analyses were conducted (* Samples were prepared from FFPE sections from the histology group).

## Energy Dispersive X-ray Spectroscopy

Consecutive formalin-fixed paraffin-embedded (FFPE) tissue sections (4 μm) of the skin and relevant brain regions, for example, GP (brain II) and DN (brain VI), of 1 animal per group were fixed with double-coated carbon conductive tabs (25-mm PLANO Leit-tabs, PLANO GmbH, Germany) on a scanning electron microscopy (SEM) cylinder specimen mounts (25-mm aluminum stubs, Agar Scientific, United Kingdom). The margins of the investigated skin and brain tissue samples were covered with copper conductive tape (PLANO GmbH, Germany) to improve the contact with the specimen mounts. The specimens were gold-coated for 100 seconds at 5 mA using a Bal-Tec SCD 005 Sputtercoater (BAL-TEC AG, Liechtenstein) and examined on a Quanta SEM 400 (FEI, Oregon) coupled to energy dispersive x-ray (EDX) spectroscopy (Genesis; EDAX, New Jersey). The sections were imaged using back-scattered electrons (atomic number contrast) and analyzed for qualitative elemental compositions of the element present; no quantitative analyses of the element concretions were conducted. All investigated specimens were scanned for the presence and number of bright z-contrast Gd-containing spots. Each slide was analyzed for 3 hours, covering approximately 25% to 30% of the surface. The observed spots were analyzed by EDX for elemental composition (Gd presence).

## Ultrastructural and SEM Evaluation of Brain and Skin

Small tissue samples were punched from the FFPE tissue of the skin and relevant brain areas (brain VI, DN) from 1 animal injected with gadodiamide or saline. The samples were stored in xylol for 3 × 1 hour, followed by incubation in decreasing ethanol concentrations (100%, 70%, 50%, and 30%) and Na-cacodylate buffer (overnight) and post-fixation in 2% osmium (3.5 hours). The samples were plastic embedded, and semi-thin sections (~1 μm thick) were cut with glass knifes, followed by staining according to Richardson et al.[30] After the light-microscopic evaluation of semi-thin sections and subsequent trimming of the plastic-embedded blocks, ultra-thin sections (0.05–0.1 μm thick) were cut and processed according to standard electron microscopic methods (uranyl acetate and lead citrate). The ultra-thin sections were mounted on copper grids. The grids were ultrastructurally evaluated using TEM-EDX coupled to energy dispersive x-ray (TEM; Tecnai 20, Fa. FEI, acceleration voltage 200 kV). The magnification applied ranged up to 191.000×. Furthermore, the SEM-EDX evaluation of semi-thin sections was performed (SEM Quanta 4001; acceleration voltage 20 kV).

## Laser Ablation-ICP-MS

To specifically visualize the tissue distribution pattern of Gd, an inductively coupled plasma mass spectrometer (Agilent 7900; Agilent Technologies, Japan) was coupled to a laser ablation system (NWR 213; New Wave Research, Fremont, CA). Brain slices were prepared as described above and embedded in Tissue Tek O.C.T. Compound (Sakura Finetek; Alphen aan den Rijn, the Netherlands) and snap frozen in isopentane. The 30-μm thick cryosections were prepared from rat brain slices containing GP (brain II) and DN (brain VI) and subsequently mounted on Superfrost Plus adhesive glass slides (Menzel Glaeser, Braunschweig, Germany). The laser ablation of biological tissue was performed as previously described[31] in continuous line ablation mode at daily optimized output energies in the range of typically 25% to 35%, with a 60-μm spot size and 30-μm residual between lines making a y-pixel dimension of 90 μm. The ablated tissue material was transported into the ICP-MS using Argon gas at a flow of 1.1 L/min. To quantify Gd in brain and skin tissue samples, matrix-matched laboratory standards of homogenized brain tissue with well-defined element concentrations were prepared and analyzed under the same conditions as the samples. Four Gd isotopes were monitored; $^{156}$Gd was used for quantification. The images were reconstructed and calibrated using an Excel algorithm and IMAGENA software for visualization.[32,33] All the analytical methods used to determine the presence and quantity of Gd species provide only information about the elemental composition of the studied object. None of the methods used is able to provide molecular information of the Gd species.

## Statistics

One-way analysis of variance (Tukey multiple comparison) test or the Kruskal-Wallis test for nonparametric analyses was used for comparisons between the groups. GraphPad Prism (GraphPad Software, La Jolla, CA) was used for all statistical analyses. The significance level was set to $P < 0.05$.

# RESULTS

## Assessment of Histological Changes in Brain and Skin Samples After GBCA Exposure

All 50 animals survived the scheduled test period (Fig. 1). No histologically evident alterations were detected in the brain at the routine histological examination of the H&E-stained slides. In addition, a more detailed examination of the areas of special interest, for example, GP, subfornicular organ (brain II), and lateral (dentate) cerebellar nucleus (brain VI, "equivalent location to the DN in humans"), using immunohistochemistry with astrocyte (GFAP) and microglia markers (Iba1) and cresyl violet staining of the Nissl substance on consecutive sections, did not reveal any adversity compared with the controls

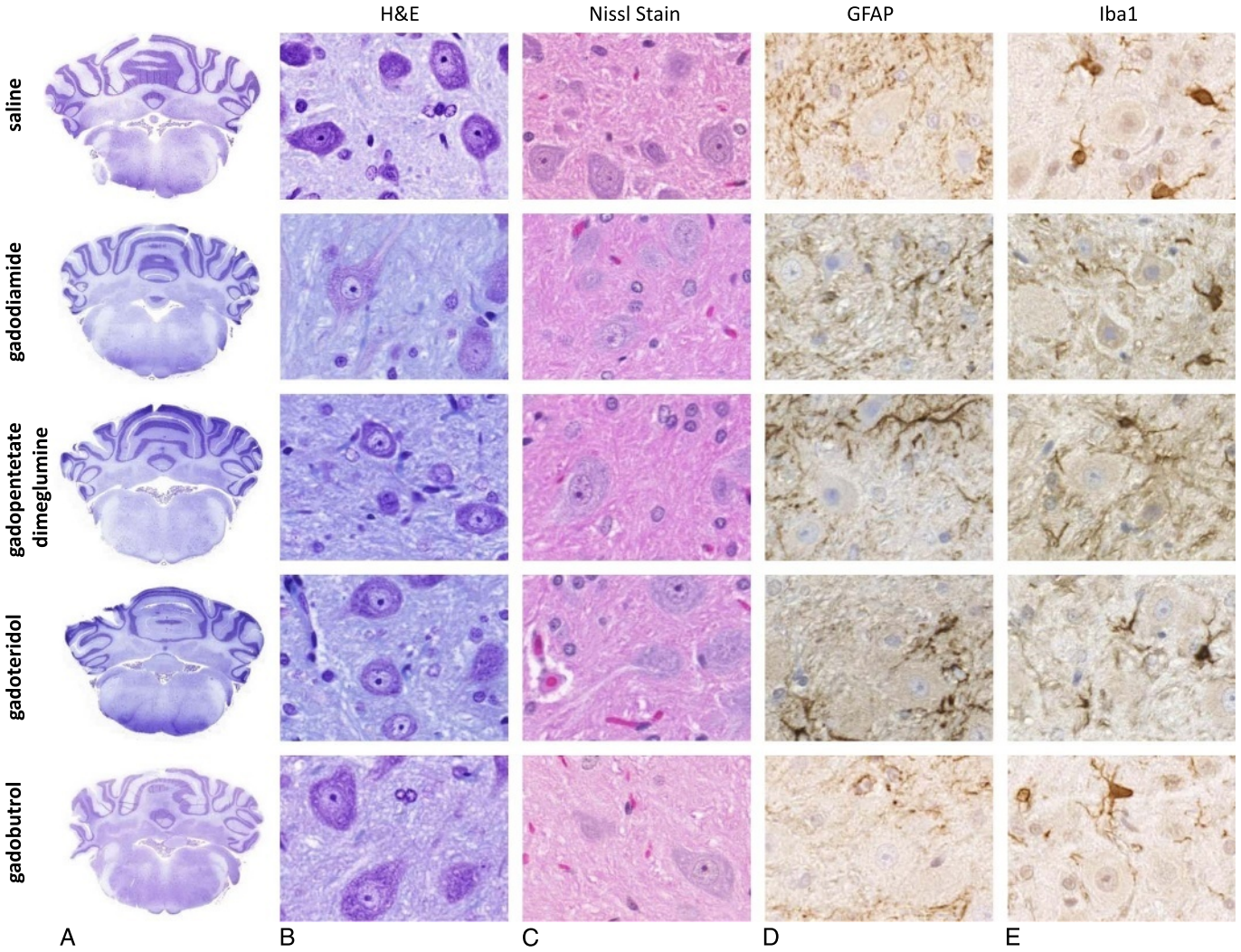


**FIGURE 2.** Despite the repeated high-dose administration of either linear or macrocyclic GBCAs (gadodiamide, gadopentetate dimeglumine, gadoteridol, gadobutrol, and control group), no histopathological changes in the brain could be detected at microscopic examination of slides stained with (A and B) H&E or (C) cresyl violet (Nissl stain). Immunohistochemistry using (D) GFAP to assess the astrocyte number and (E) morphology, and a microglial marker (Iba1) did not reveal any differences between animals administered linear or macrocyclic GBCAs compared with vehicle controls.

(Fig. 2). A single Gd-positive domain could be detected in the neutrophil of a 4-μm thick brain section of 1 animal administered gadodiamide using SEM-EDX (data not shown). Semi-thin sections (~1 μm) of the brains of animals administered gadodiamide did not show any positive signals in any of the specimens that were investigated. By contrast, several positive signals for Gd were observed at a higher magnification of an ultra-thin section (0.05–0.1 μm) during TEM evaluation (Fig. 3). The microscopic examination of the semithin sections and the electron microscopic examination of the ultrathin sections revealed a regular tissue architecture with the neurons, glial cells, and focally typical cerebellar structure (granular and Purkinje cells) in animals administered gadodiamide and saline. The electron-dense signals in TEM (dark spots) generally occurred as a single focus or rarely as multiple roundish nodules with variable diameters up to a size of 0.5 μm (Fig. 3, A and B). Energy dispersive x-ray analysis clearly detected Gd-positive signals in these electron-dense areas (Fig. 3D). The EDX spectrum of these areas in the brain during TEM evaluation was similar to the Gd-positive signal of the skin during SEM evaluation in the same rat (see Supplementary Figure, Supplemental Digital Content 1, http://links.lww.com/RLI/A304).

Four of 10 animals intravenously injected with gadodiamide showed macroscopic NSF-like skin lesions, histologically correlated with fibrosis and mononuclear cell infiltration (Fig. 4). No adverse effects were detected in the skin of animals administered saline, linear gadopentetate dimeglumine, or macrocyclic gadoteridol and gadobutrol. Energy dispersive x-ray spectroscopy was applied to analyze the elemental composition, including the presence of Gd in the skin on serial sections. The presence of Gd-containing domains in the connective tissue of the subcutis was only observed for both linear agents with gadodiamide having approximately 3- to 4-fold more Gd domains in the skin than linear gadopentetate dimeglumine (Fig. 5).

## Gadolinium Quantification in Skin, Bone, Brain, and Muscle

The effect of high doses of GBCAs (administered intravenously) on the amount of residual Gd in skin, bone, skeletal muscle, and brain tissue was assessed using ICP-MS (Fig. 6). Eight weeks after the last injection, the highest Gd concentration was measured after the administration of linear gadodiamide (1472 ± 115 nmol Gd/g

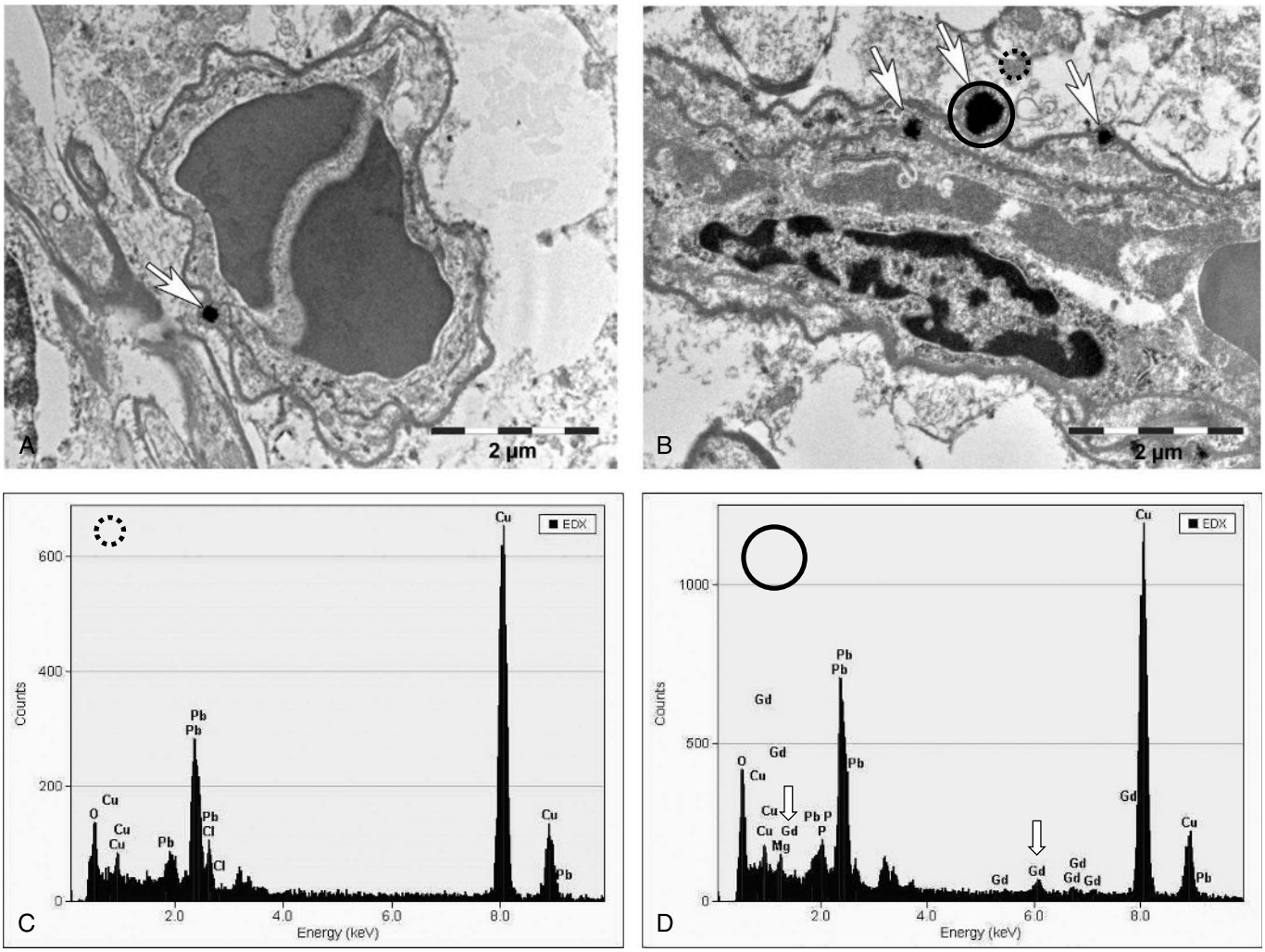


**FIGURE 3.** Transmission electron microscopy tissue localization of Gd-containing spots in the region of the lateral (dentate) cerebellar nuclei in the brain after the repeated high-dose application of gadodiamide (20 × 2.5 mmol Gd/kg body weight). TEM evaluation showed several positive signals: (A) 1 single focus (original magnification, ×18,900) and (B) several electron-dense signals occurring as multiple roundish nodules with variable diameter (original magnification, ×18,800). The location indicates intracellular deposition within endothelial cell of blood vessels; 1 signal appeared to be adjacent to an endothelial cell on the adluminal side. The EDX analysis showed, compared with the control area (C), Gd-positive signals (D, arrows). No positive signals could be detected in neurons or in the neuropil.

tissue), followed by linear gadopentetate dimeglumine (80.8 ± 6.2 nmol Gd/g tissue) in the skin (and bone) of rats. By contrast, the amount of measured Gd in the skin after macrocyclic gadobutrol and gadoteridol administration was extremely low, with 1.1 ± 0.5 and 1.7 ± 0.8 nmol Gd/g tissue, respectively (Fig. 6A).

The average concentration of residual Gd in the brain was approximately 15-fold higher for linear than for macrocyclic GBCAs (Fig. 6B). Animals administered linear gadodiamide and gadopentetate dimeglumine displayed significantly higher Gd concentrations in the brain, 11.1 ± 5.1 and 13.1 ± 7.3 nmol Gd/g tissue, whereas 0.7 ± 0.4 and 0.5 ± 0.2 nmol Gd/g tissue was detected in the brains of animals administered macrocyclic gadobutrol and gadoteridol, respectively. However, the overall amount of Gd observed in the brain after linear GBCA administration remained extremely low, with 0.0002% of the injected dose per gram of tissue. The Gd concentrations in the brain were approximately 100-fold less compared with the skin. The detected Gd concentrations in 7 dissected brain samples (brain I-VII) showed no significant preferential anatomical location for Gd such as GP (brain II) or lateral (dentate) cerebellar nucleus (brain VI) (Fig. 7). Interestingly, the highest Gd concentration in the brain was detected in the olfactory bulb (brain I) and decreased in the posterior direction in animals administered gadopentetate dimeglumine, whereas the concentration of Gd was similar in all investigated 7 brain regions of animals administered gadodiamide (Fig. 7).

## Gadolinium Distribution in Brain and Skin Tissue

The impact of multiple administrations of linear and macrocyclic GBCAs on the distribution pattern of Gd in brain and skin cryosections was analyzed using laser ablation ICP-MS (LA-ICP-MS) (Fig. 8). In line with the ICP-MS data that were shown previously (Figs. 6, 7), the spatially resolved LA-ICP-MS measurements displayed the highest Gd signals in skin and brain tissue after the administration of linear GBCAs gadodiamide and gadopentetate dimeglumine. According to the concentration scale, which ranged from 0 to 100 mg Gd/kg for skin and 0 to 4 mg Gd/kg for brain, the highest Gd values were observed in the skin and deep cerebellar nuclei of rats administered gadodiamide and to a lesser extent, with gadopentetate dimeglumine. In addition to the specific localization in the deep cerebellar nuclei, substantial Gd

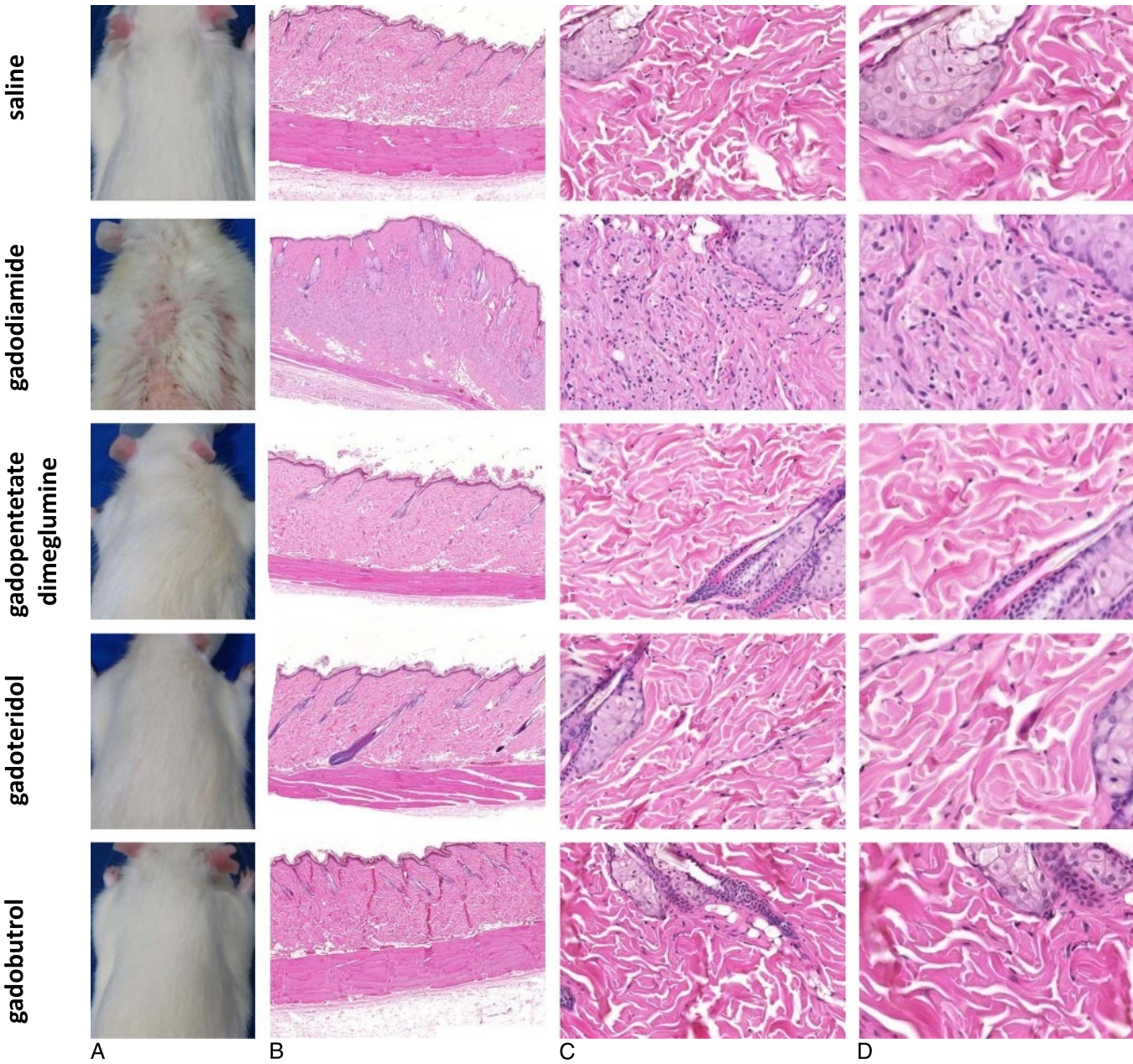


**FIGURE 4.** A, Macroscopic skin appearance and (B) an overview of the skin tissue and (C and D) enlarged H&E skin sections of animals administered saline, gadodiamide, gadopentetate dimeglumine, gadoteridol, and gadobutrol. Representative H&E-stained FFPE sections of animals, each injected with 20 injections at a dose of 2.5 mmol Gd/kg body weight at 8 weeks after the last injection. All animals in the gadodiamide group showed fibrosis and mononuclear cell infiltration and an increase in dermal cellularity compared with the saline group and all other investigated groups.

signals could also be visualized in other brain regions such as the granular layer of the cerebellar cortex. In all brains from linear and macrocyclic GBCAs groups, very low and homogeneous, background-like distribution of Gd was observed. However, it is important to note that a local accumulation of Gd within the deep cerebellar nuclei and the granular layer was observed only with linear agents (Fig. 8).

## DISCUSSION

No histological changes were detected in the brain after multiple administrations of either linear or macrocyclic GBCAs (Fig. 2). These findings are consistent with preclinical and the few available clinical data reporting the lack of apparent histological changes in H&E-stained sections of DN from rats and patients administered gadodiamide.[10,34] Despite the absence of obvious GBCA-mediated histopathological changes in the brain, varying Gd concentrations in the brain were measured using ICP-MS. Compared with macrocyclic GBCA administration, the Gd concentration measured in the brain was approximately 15 times higher when linear GBCAs were administered. These findings are consistent with previous preclinical studies showing that the amount of Gd detected in brain tissue samples was significantly higher for linear than for macrocyclic GBCAs.[22,23,35,36]

Using spatially resolved LA-ICP-MS, very low and homogeneously distributed Gd concentrations in the brain were measurable for

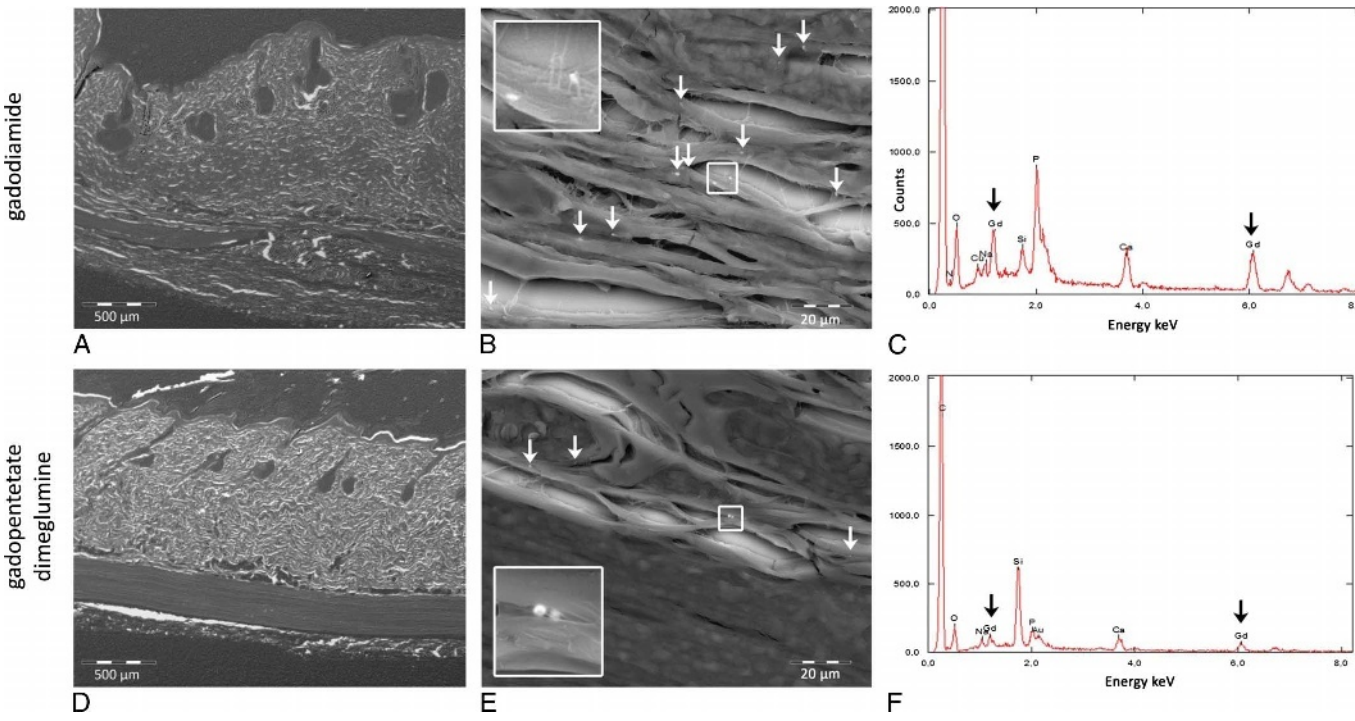


**FIGURE 5.** Scanning electron microscopy coupled to energy dispersive x-ray (SEM-EDX) spectroscopy for the detection of elemental composition, including Gd presence in the skin after the application of 20 injections (2.5 mmol Gd/kg body weight) of the linear agents gadodiamide and gadopentetate dimeglumine. A, An overview of the skin tissue (original magnification, ×50), (B) an enlarged skin section (original magnification, ×1000), and (C) the presence of Gd-containing domains in the connective tissue of the subcutis. The gadodiamide-injected rat (upper row) showed approximately 3 to 4 times more Gd domains in the skin than the gadopentetate dimeglumine-administered rat (lower row).

both classes of GBCAs like a background signal. High Gd concentrations were detected in the deep cerebellar nuclei of rats only after the repeated high-dose application of linear GBCAs. Interestingly, Gd was detected in additional brain regions, such as the granular layer of the cerebellar cortex, but in these regions, the local accumulation of Gd was only present for linear agents (Fig. 8). In contrast to the DN, no increased signal intensities in the granular layer of the cerebellar cortex has been reported in clinical or nonclinical studies while the LA-ICP-MS clearly shows the presence of Gd in rats treated with linear GBCAs. One possible explanation for this observation could be that Gd is under a distinct form in the cerebellar cortex (eg, insoluble and nonvisible in the MRI) and in the cerebellar nuclei (eg, high-relaxivity Gd bound to a macromolecule).

Moreover, Gd-positive high electron-dense structures in TEM, specifically located in the wall of several microvessels in the brain of a rat administered gadodiamide, confirm these findings and are consistent with the results of McDonald et al[10] in humans (Fig. 3). The Gd-positive high electron-dense structures in TEM could only be detected in the endothelial wall of several microvessels in the brain of 1 gadodiamide administered rat and not in neurons, neutrophil, or other glial cells, raising the possibility that Gd may not have passed the BBB. This finding has to be further examined on more samples and animals, as well as after the administration of other GBCAs than gadodiamide.

Consistent with previously published preclinical NSF studies,[3,37] some of the animals injected with gadodiamide but none of the other groups showed macroscopically and histologically NSF-like skin lesions (Fig. 4). Despite the limitations of animal models in general, these findings suggest that the preclinical studies in the rat reliably mimic effects, at least in the skin, that appear to be associated with GBCA

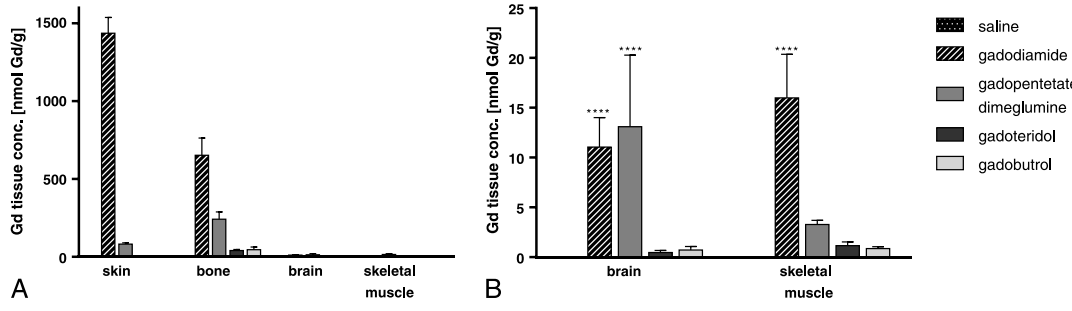


**FIGURE 6.** A, Eight weeks after the last injection (20 × 2.5 mmol Gd/kg body weight), high Gd concentrations were measured for the linear agents gadodiamide and gadopentetate dimeglumine in the skin and bone. B, The average concentration (mean ± SD) of residual Gd in the brain was approximately 100-fold lower compared with the skin in gadodiamide-injected rats and approximately 15-fold higher for linear than for macrocyclic GBCAs. Low Gd concentrations were measurable when both classes of GBCAs were used.

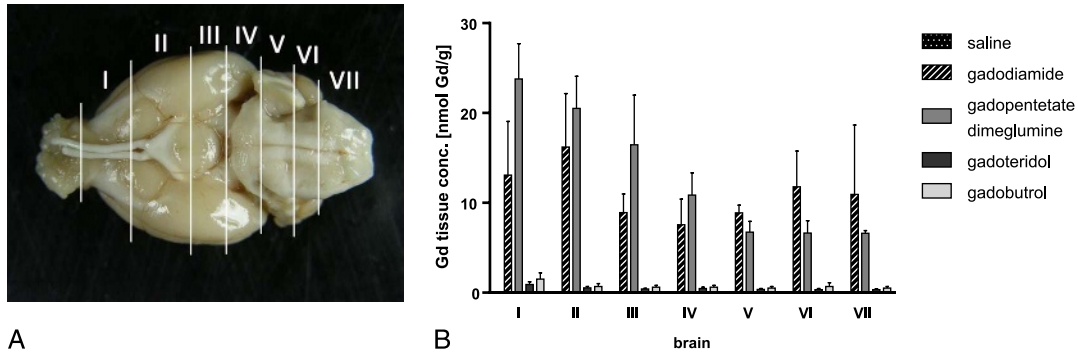


**FIGURE 7.** A, Seven different brain sections (brain I-VII) were investigated. The Gd concentrations in the 7 dissected brain samples showed no significant preferential anatomical location of Gd, such as the GP (brain II) or lateral (dentate) cerebellar nucleus (brain VI). B, Interestingly, the highest Gd concentration in the brain was detected in the olfactory bulb (brain I) decreasing in the posterior direction in animals administered gadopentetate dimeglumine, whereas the concentration of Gd was similar in all 7 investigated brain regions of animals administered with gadodiamide. All values are given as mean ± SD.

stability. In addition, Robert et al[22,23] and Jost et al[21] showed that multiple injections of extended doses of GBCAs mimic the clinical observation of increased signal intensities within the deep cerebellar nuclei on MRI. Therefore, the rat is considered a suitable species to evaluate the potential effects of GBCAs in the brain.

The presence of small traces of residual Gd in the brain with an intact BBB raises several questions and challenges the current knowledge of the biodistribution of GBCAs. The underlying mechanism of Gd presence in the brain is not yet known. Two hypotheses for the increased signal intensity in the brain have been discussed in the

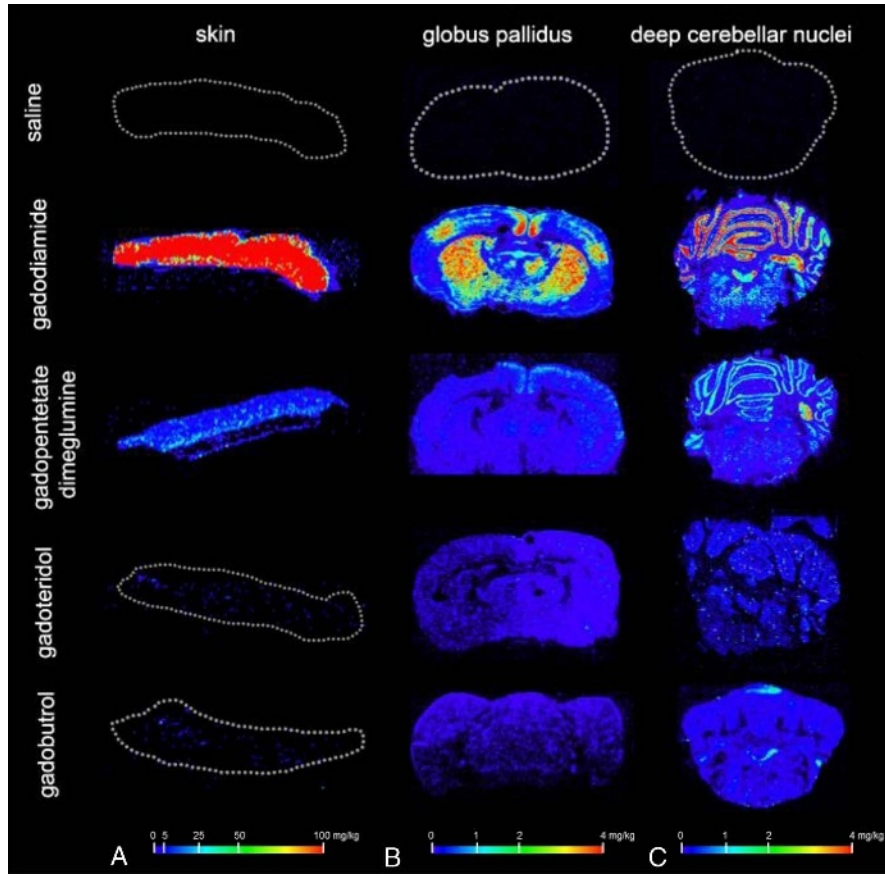


**FIGURE 8.** Tissue distribution after repeated high-dose administration of saline, gadodiamide, gadopentetate dimeglumine, gadobutrol, and gadoteridol measured using laser ablation ICP-MS. The highest Gd signals were detected in the (A) skin, (B) GP region, and (C) deep cerebellar nuclei region after the administration of the linear GBCAs gadodiamide and gadopentetate dimeglumine. In addition to the specific localization in the deep cerebellar nuclei, substantial Gd signals could also be visualized in other brain regions, such as the granular layer of the cerebellar cortex and in the facial nuclei in the pons. No local accumulation of Gd was observed within the deep cerebellar nuclei and the granular layer after the administration of macrocyclic gadobutrol and gadoteridol.

literature: the recirculation from "reservoirs" (such as bone)[38,39] and the progressive alteration of the Gd chelate, from a low-relaxivity (eg, intact GBCA) to a high-relaxivity molecule (eg, Gd bound to a macromolecule).[40] As the high Gd concentrations in the skin and bone of animals administered with gadodiamide did not increase the levels of Gd in the brain compared with gadopentetate dimeglumine, a potential recirculation from "reservoirs" seems unlikely. However, the finding that the highest Gd concentrations in the deep cerebellar nuclei were measured up to 4 mg of Gd/kg (25.4 μmol Gd/kg tissue) supports the second hypothesis because a robust contrast enhancement requires a GBCA concentration of approximately 125 μmol Gd/L[41] and Wedeking et al[42] evaluated 30 μmol Gd/L as the MRI detection limit.

After linear GBCA administration, only 0.0002% ID per gram of the injected dose was detected in the brain. This is similar to recently published data[34] and below the detection limit (0.004% ± 0.001% ID/g) of a formerly published work investigating $^{153}$Gd-radiolabeled long-term Gd distribution of different contrast agents in both mice and rats.[43] Nevertheless, how small amounts of GBCAs enter the brain remains unknown. Jost et al showed cerebrospinal fluid (CSF) enhancement independently of the different GBCA classes (linear or macrocyclic and ionic or nonionic) using highly sensitive T2-weighted FLAIR sequences.[21] Small amounts of GBCAs might be transported into the CSF via the choroid plexus because the blood-CSF barrier is leakier than the BBB.[44,45] In a recently published study in healthy rats, Jost et al[46] showed a hyperintense CSF using a sensitive FLAIR sequence and measured 4.5 hours after GBCA administration of a CSF concentration up to a maximum of 27.4 nmol Gd/mL by ICP-MS, which is equivalent to 0.006% ID/g. In humans, 500 mL of CSF is secreted at the choroid plexus each day, which is further distributed into the subarachnoid space and subsequently into the blood via bulk flow, consistent with many drug substances distributed into the CSF.[44] Iliff et al[47] showed that after intracisternal injection, GBCAs distribute along the glymphatic system, a so-called waste clearance system, from the basal artery to the olfactory artery (paravascular pathway), suggesting that GBCAs enter the brain through the exchange between cerebrospinal and interstitial fluid (CSF-ISF exchange).[48] It was further suggested that the exchange of CSF and ISF between the paravascular space and the neuropil across the perivascular astrocytic end-feet depends on the molecular size (molecular weight) of the molecule. These studies reported that small molecules readily pass into and through the neuropil, whereas large molecules remain in paravascular spaces.[47] Gd ions derived from partial dissociation of GBCAs would not exist in free form in any significant amounts in the physiological environment, because of the presence of a multitude of high affinity binding partners, such as proteins, peptides, or inorganic phosphate or carbonate with very low solubility. The potential macromolecular binding partner and the Gd species responsible for the high MR signal intensity have not yet been identified, but potential binding partners are glucosaminoglycanes,[40] transferrin,[49] or parvalbumin.[50] Further studies are required to clarify how and to what extent transmetallation of the Gd from the intact GBCA to other binding partners/ligands might occur. However, the formation of macromolecular Gd complexes might subsequently delay the efficient and fast clearance from the brain via the glymphatic system.[47]

Recently, a preclinical study from Kartamihardja et al[35] explored the concentration and clearance of retained Gd in various parts of the brain after linear and macrocyclic GBCA administration in normal and renal failure mouse models. These authors reported that the Gd concentration was highest in the olfactory bulb of both GBCA classes. Interestingly, they showed that the Gd deposits from macrocyclic gadoterate meglumine were eliminated from the brain over time, whereas a significant amount of Gd from linear gadodiamide remained in all assessed parts of the brain under normal and renal failure conditions. In accordance with the results of Kartamihardja et al,[35] the highest Gd concentration was observed in the olfactory bulb of animals administered linear GBCAs gadopentetate dimeglumine, suggesting an ongoing drainage of CSF from the subarachnoid space through the olfactory nerves into the nasal lymphatic system.

However, the measured Gd concentrations in the brain are significantly lower compared with the skin and nearly comparable with the skeletal muscles. Moreover, the present histological study did not show any morphological changes or obvious tissue reactions such as degeneration or inflammation.

Certain technical and procedural limitations of this study exist. First, the method used for measuring Gd cannot distinguish between chelated and dechelated Gd, and therefore, it is not possible to precisely determine whether the measured residual Gd is chelated or dechelated after the administration of linear GBCAs. Second, at least 2 different time points should be investigated to analyze Gd retention over a certain period to assess a potential wash-out effect, clearance, or precipitation of Gd, which was beyond the scope of the present study. Furthermore, the low n (n = 3) limits statistical analysis and only 4 of the 9 marketed GBCAs were investigated in the present study. In addition, the interval between the 20 consecutive injections and the time between the last injection and the MRI significantly differed from clinical studies, as did the dose. Transmission electron microscopy (ultra-thin sections, 0.05–0.1 μm thick) was not applied for all the investigated groups, as this analysis is on the one hand expensive and time-consuming and on the other hand, the LA-ICP-MS analysis using 30-μm sections is more sensitive and facilitates semiquantitative Gd detection.

The data presented in the present study contribute to a better understanding of how Gd is distributed within the brain and skin depending on the class of GBCA administered (linear vs macrocyclic). Based on these findings, we propose that Gd chelate stability plays an important role in the deposition of Gd in various tissues and organs. The differences in Gd chelate stability are well known and have repeatedly been shown.[2,6] Currently, there is a growing body of evidence from clinical[9,11,13–17,51] and preclinical studies[21–23,35,36] suggesting that the potential of a GBCA to increase SI and presumably Gd retention in the brain depends on its specific stability.[52,53] Nevertheless, further scientific investigations are needed to elucidate the precise mechanism of how GBCAs enter the brain.

However, it is important to keep in mind that contrast-enhanced MRI scans fulfill important medical needs, thereby improving the accuracy of diagnoses, and that they aid in treatment decisions. The verified safety profiles for GBCAs have been established over decades and are based on in-depth medical experiences and many millions of administrations. The hyperintensity or presence of Gd in the brain has not been associated with any adverse health effects. Still, both the mechanisms and potential clinical relevance of these findings warrant further investigation.

## ACKNOWLEDGMENTS

*The authors would like to thank Ines Krause, Robert Ivkic, David Hallmann, Christine Ludwig, Michael Hasbach, Hansgeorg Rückert, Sabina Bassow, Viola Neumeyer, and Nicola Knabenreich for their motivation, excellent work, and technical assistance, and Joachim Neumann and Matthias Voetz, PhD (Bayer Technology Services GmbH) for the assistance with the comprehensive SEM-EDX measurements. The authors would also like to thank Wolfgang Ebert, PhD, for constructive discussions and critical reading of the manuscript.*

## REFERENCES

1. Lohrke J, Frenzel T, Endrikat J, et al. 25 years of contrast-enhanced MRI: developments, current challenges and future perspectives. *Adv Ther*. 2016;33:1–28.
2. Frenzel T, Lengsfeld P, Schirmer H, et al. Stability of gadolinium-based magnetic resonance imaging contrast agents in human serum at 37 degrees C. *Invest Radiol*. 2008;43:817–828.
3. Sieber MA, Lengsfeld P, Frenzel T, et al. Preclinical investigation to compare different gadolinium-based contrast agents regarding their propensity to release

gadolinium in vivo and to trigger nephrogenic systemic fibrosis-like lesions. *Eur Radiol*. 2008;18:2164–2173.

4. Morcos SK. Nephrogenic systemic fibrosis following the administration of extracellular gadolinium based contrast agents: is the stability of the contrast agent molecule an important factor in the pathogenesis of this condition? *Br J Radiol*. 2007; 80:73–76.
5. Khurana A, Runge VM, Narayanan M, et al. Nephrogenic systemic fibrosis: a review of 6 cases temporally related to gadodiamide injection (Omniscan). *Invest Radiol*. 2007;42:139–145.
6. Schmitt-Willich H. Stability of linear and macrocyclic gadolinium based contrast agents. *Br J Radiol*. 2007;80:581–582; author reply 584–585.
7. Thomsen HS, Morcos SK, Almén T, et al. Nephrogenic systemic fibrosis and gadolinium-based contrast media: updated ESUR Contrast Medium Safety Committee guidelines. *Eur Radiol*. 2013;23:307–318.
8. Kanda T, Ishii K, Kawaguchi H, et al. High signal intensity in the dentate nucleus and globus pallidus on unenhanced T1-weighted MR images: relationship with increasing cumulative dose of a gadolinium-based contrast material. *Radiology*. 2014;270:834–841.
9. Errante Y, Cirimele V, Mallio CA, et al. Progressive increase of T1 signal intensity of the dentate nucleus on unenhanced magnetic resonance images is associated with cumulative doses of intravenously administered gadodiamide in patients with normal renal function, suggesting dechelation. *Invest Radiol*. 2014;49:685–690.
10. McDonald RJ, McDonald JS, Kallmes DF, et al. Intracranial gadolinium deposition after contrast-enhanced MR imaging. *Radiology*. 2015;275:772–782.
11. Kanda T, Osawa M, Oba H, et al. High signal intensity in dentate nucleus on unenhanced T1-weighted MR images: association with linear versus macrocyclic gadolinium chelate administration. *Radiology*. 2015;275:803–809.
12. Adin ME, Kleinberg L, Vaidya D, et al. Hyperintense dentate nuclei on T1-weighted MRI: relation to repeat gadolinium administration. *AJNR Am J Neuroradiol*. 2015;36:1859–1865.
13. Radbruch A, Weberling LD, Kieslich PJ, et al. Gadolinium retention in the dentate nucleus and globus pallidus is dependent on the class of contrast agent. *Radiology*. 2015;275:783–791.
14. Cao Y, Huang DQ, Shih G, et al. Signal change in the dentate nucleus on T1-weighted MR images after multiple administrations of gadopentetate dimeglumine versus gadobutrol. *AJR Am J Roentgenol*. 2016;206:414–419.
15. Weberling LD, Kieslich PJ, Kickingereder P, et al. Increased signal intensity in the dentate nucleus on unenhanced T1-Weighted images after gadobenate dimeglumine administration. *Invest Radiol*. 2015;50:743–748.
16. Ramalho J, Castillo M, AlObaidy M, et al. High signal intensity in globus pallidus and dentate nucleus on unenhanced T1-weighted MR images: evaluation of two linear gadolinium-based contrast agents. *Radiology*. 2015;276:836–844.
17. Radbruch A, Weberling LD, Kieslich PJ, et al. High-signal intensity in the dentate nucleus and globus pallidus on unenhanced T1-weighted images: evaluation of the macrocyclic gadolinium-based contrast agent gadobutrol. *Invest Radiol*. 2015;50:805–810.
18. Kanda T, Fukusato T, Matsuda M, et al. Gadolinium-based contrast agent accumulates in the brain even in subjects without severe renal dysfunction: evaluation of autopsy brain specimens with inductively coupled plasma mass spectroscopy. *Radiology*. 2015;276:228–232.
19. Semelka RC, Ramalho M, AlObaidy M, et al. Gadolinium in humans: a family of disorders. *AJR Am J Roentgenol*. 2016;207:229–233.
20. Burke LM, Ramalho M, AlObaidy M, et al. Self-reported gadolinium toxicity: a survey of patients with chronic symptoms. *Magn Reson Imaging*. 2016;34: 1078–1080.
21. Jost G, Lenhard DC, Sieber MA, et al. Signal increase on unenhanced T1-weighted images in the rat brain after repeated, extended doses of gadolinium-based contrast agents: comparison of linear and macrocyclic agents. *Invest Radiol*. 2016;51:83–89.
22. Robert P, Lehericy S, Grand S, et al. T1-weighted hypersignal in the deep cerebellar nuclei after repeated administrations of gadolinium-based contrast agents in healthy rats: difference between linear and macrocyclic agents. *Invest Radiol*. 2015;50:473–480.
23. Robert P, Violas X, Grand S, et al. Linear gadolinium-based contrast agents are associated with brain gadolinium retention in healthy rats. *Invest Radiol*. 2016;51:73–82.
24. Bolon B, Garman RH, Pardo ID, et al. STP position paper: recommended practices for sampling and processing the nervous system (brain, spinal cord, nerve, and eye) during nonclinical general toxicity studies. *Toxicol Pathol*. 2013;41:1028–1048.
25. Duchen LW. Current status review: cerebral amyloid. *Int J Exp Pathol*. 1992;73: 535–550.
26. Kaufmann W, Bolon B, Bradley A, et al. Proliferative and nonproliferative lesions of the rat and mouse central and peripheral nervous systems. *Toxicol Pathol*. 2012; 40(suppl 4):87S–157S.
27. Keaney J, Campbell M. The dynamic blood-brain barrier. *FEBS J*. 2015;282:4067–4079.
28. Crissman JW, Goodman DG, Hildebrandt PK, et al. Best practices guideline: toxicologic histopathology. *Toxicol Pathol*. 2004;32:126–131.
29. Neef N, Nikula KJ, Francke-Carroll S, et al. Regulatory forum opinion piece: blind reading of histopathology slides in general toxicology studies. *Toxicol Pathol*. 2012;40:697–699.
30. Richardson KC, Jarett L, Finke EH. Embedding in epoxy resins for ultrathin sectioning in electron microscopy. *Stain Technol*. 1960;35:313–323.
31. M-M P, Weiskirchen R, Gassler N, et al. Novel bioimaging techniques of metals by laser ablation inductively coupled plasma mass spectrometry for diagnosis of fibrotic and cirrhotic liver disorders. *PLoS One*. 2013;8:e58702.
32. Boaru SG, Merle U, Uerlings R, et al. Simultaneous monitoring of cerebral metal accumulation in an experimental model of Wilson's disease by laser ablation inductively coupled plasma mass spectrometry. *BMC Neurosci*. 2014;15:98.
33. Osterholt T, Salber D, Matusch A, et al. IMAGENA: Image Generation and Analysis—An interactive software tool handling LA-ICP-MS data. *Int J Mass Spectrom*. 2011;307:232–239.
34. Smith AP, Marino M, Roberts J, et al. Clearance of gadolinium from the brain with no pathologic effect after repeated administration of gadodiamide in healthy rats: an analytical and histologic study. *Radiology*. 2016.
35. Kartamihardja AA, Nakajima T, Kameo S, et al. Distribution and clearance of retained gadolinium in the brain: differences between linear and macrocyclic gadolinium based contrast agents in a mouse model. *Br J Radiol*. 2016;89:20160509.
36. Kartamihardja AA, Nakajima T, Kameo S, et al. Impact of impaired renal function on gadolinium retention after administration of gadolinium-based contrast agents in a mouse model. *Invest Radiol*. 2016;51:655–660.
37. Pietsch H, Lengsfeld P, Jost G, et al. Long-term retention of gadolinium in the skin of rodents following the administration of gadolinium-based contrast agents. *Eur Radiol*. 2009;19:1417–1424.
38. Lancelot E. Revisiting the pharmacokinetic profiles of gadolinium-based contrast agents: differences in long-term biodistribution and excretion. *Invest Radiol*. 2016;51:691–700.
39. Hirano S, Suzuki KT. Exposure, metabolism, and toxicity of rare earths and related compounds. *Environ Health Perspect*. 1996;104(suppl 1):85–95.
40. Taupitz M, Stolzenburg N, Ebert M, et al. Gadolinium-containing magnetic resonance contrast media: investigation on the possible transchelation of Gd(3)(+) to the glycosaminoglycan heparin. *Contrast Media Mol Imaging*. 2013;8:108–116.
41. Caravan P. Strategies for increasing the sensitivity of gadolinium based MRI contrast agents. *Chem Soc Rev*. 2006;35:512–523.
42. Wedeking P, Shukla R, Kouch YT, et al. Utilization of the nephrectomized mouse for determining threshold effects of MRI contrast agents. *Magn Reson Imaging*. 1999;17:569–575.
43. Tweedle MF, Wedeking P, Kumar K. Biodistribution of radiolabeled, formulated gadopentetate, gadoteridol, gadoterate, and gadodiamide in mice and rats. *Invest Radiol*. 1995;30:372–380.
44. Pardridge WM. Drug transport in brain via the cerebrospinal fluid. *Fluids Barriers CNS*. 2011;8:7.
45. Levy LM. Exceeding the limits of the normal blood-brain barrier: quo vadis gadolinium? *AJNR Am J Neuroradiol*. 2007;28:1835–1836.
46. Jost G, Frenzel T, Lohrke J, et al. Penetration and distribution of gadolinium-based contrast agents into the cerebrospinal fluid in healthy rats: a potential pathway of entry into the brain tissue. *Eur Radiol*. 2016.
47. Iliff JJ, Lee H, Yu M, et al. Brain-wide pathway for waste clearance captured by contrast-enhanced MRI. *J Clin Invest*. 2013;123:1299–1309.
48. Jessen NA, Munk AS, Lundgaard I, et al. The glymphatic system: a beginner's guide. *Neurochem Res*. 2015;40:2583–2599.
49. Korkusuz H, Ulbrich K, Welzel K, et al. Transferrin-coated gadolinium nanoparticles as MRI contrast agent. *Mol Imaging Biol*. 2013;15:148–154.
50. Xue S, Yang H, Qiao J, et al. Protein MRI contrast agent with unprecedented metal selectivity and sensitivity for liver cancer imaging. *Proc Natl Acad Sci U S A*. 2015;112:6607–6612.
51. Quattrocchi CC, Mallio CA, Errante Y, et al. Gadodiamide and dentate nucleus T1 hyperintensity in patients with meningioma evaluated by multiple follow-up contrast-enhanced magnetic resonance examinations with no systemic interval therapy. *Invest Radiol*. 2015;50:470–472.
52. Runge VM. Safety of the gadolinium-based contrast agents for magnetic resonance imaging, focusing in part on their accumulation in the brain and especially the dentate nucleus. *Invest Radiol*. 2016;51:273–279.
53. Runge VM. Commentary on T1-weighted hypersignal in the deep cerebellar nuclei after repeated administrations of gadolinium-based contrast agents in healthy rats: difference between linear and macrocyclic agents. *Invest Radiol*. 2015;50: 481–482.